Hyperfine structure of ^{14}N II $2p3p\ ^1P_1$ after ion-beam surface interaction at grazing incidence

H. Winter and H. J. Andrä
Fachbereich Physik der Freien Universität Berlin, Boltzmannstrasse 20, 1000 Berlin 33, West Germany
(Received 16 July 1979)

The high degree of orientation of atomic angular momentum states obtained by the interaction of fast ions with a solid surface at grazing incidence allows the application of the zero-field quantum-beat technique for high-resolution studies in atomic spectroscopy. With this new technique the authors have measured the hyperfine splitting of ^{14}N II $2p3p\ ^1P_1$ and deduce for the hyperfine constants values of $A = 102.9 \pm 1.0$ MHz and $B = -4.58 \pm 0.05$ MHz, and for the quadrupole moment $Q(^{14}\mathrm{N}) = 19.3 \pm 0.8$ mb.

I. INTRODUCTION

Observation of zero-field quantum beats after the excitation of a fast ion beam is a powerful method in high-resolution atomic spectroscopy.[1] The conditions for the application of this technique are the coherent excitation of fine or hyperfine (hf) levels and an anisotropic sublevel population. The different kinds of excitation media (foil, gas-target, laser) usually fulfill these conditions. Excitation of an ion beam with a crossed laser beam works only in those cases where the transitions from ground or metastable states lie in the domain of currently available laser wavelengths. On the other hand, excitation by a foil or gas lacks sufficient anisotropy for high-resolution studies in heavier atoms (tilting the foil produces an orientation of atomic states and improves the situation).

Since the ion-beam surface interaction at grazing incidence (IBSIGI) produces large degrees of orientation of atomic angular momentum states,[2] the coherence and anisotropy inherent in this kind of light source guarantees a wide range of applicability for high-resolution studies in atomic spectroscopy.

In recent papers different IBSIGI techniques for hyperfine studies have been described which allow investigations of atomic and ionic states which have been inaccessible to previously known techniques.[3,4]

In continuing the former work[4] we show that the degree of precision of data by IBSIGI quantum beats is comparable to other high-resolution techniques. We describe in this paper the study of the hyperfine structure (hfs) of the N II $1s^2 2s^2 2p3p\ ^1P_1$ state via zero-field quantum beats in the fluorescence of circularly polarized light emitted after ion-surface interaction.

In Sec. II we first discuss some aspects of the application of this new technique. We then present in Sec. III a description of the experimental setup followed by the actual measurements in Sec. IV. Since the conversion of the results obtained in Sec. V into the frequency domain requires knowledge of the average ion velocity, we devote Sec. VI to the extensive determination of this velocity. We then extract the nuclear quadrupole moment of ^{14}N from our hfs data in Sec. VII, compare it with previously reported values, and conclude with general remarks relevant to the future application of our technique in Sec. VIII.

II. QUANTUM BEATS

The time dependence of the intensity of light of wave vector $\vec{k}$ and polarization $\vec{\epsilon}$ is given by expressions in the appendix of Ref. 1. With the excitation-density tensor components in LM_L subspace ${}^{LL}\rho_q^k$, the polarization-density tensor components $\phi_q^k(\vec{k}, \vec{\epsilon})$, $\omega_{JF_1F_2} = \omega_{JF_1} - \omega_{JF_2}$, and L_0 referring to the angular momentum of the lower state, we have

$$I(\vec{k}, \vec{\epsilon}, t) \simeq \sum_{kq} (-1)^{1+L+L_0} \begin{Bmatrix} 1 & 1 & k \\ L & L & L_0 \end{Bmatrix} \phi_q^k(\vec{k}, \vec{\epsilon})\, {}^{LL}\rho_q^k(0)\, |\langle L \| \gamma Y^1 \| L_0 \rangle|^2 \times \sum_{JF_1F_2} \frac{(2J+1)^2(2F_1+1)(2F_2+1)}{(2I+1)(2S+1)} \begin{Bmatrix} J & J & k \\ L & L & S \end{Bmatrix}^2 \begin{Bmatrix} F_1 & F_2 & k \\ J & J & I \end{Bmatrix}^2 \exp(-i\omega_{JF_1F_2} t - \gamma t)\,. \quad (1)$$

The highly oriented states prepared by IBSIGI correspond to tensorial components with $k = 1$; the alignment is usually small so that $k = 2$ contributions are neglected. From the last $6j$ symbol in Eq. (1), it follows that frequencies corresponding to the hf splittings of states with $\Delta F = F_2 - F_1 = \pm 1$ are observable in the circularly polarized fluorescent light. This results, for the ^{14}N II $2p3p\ ^1P_1$

state (nuclear spin $I=1$), in two observable frequencies in the modulation of the decay.

Because of the finite length of the presumably square-shaped excitation (δx) and detection zone (Δx), one must modify Eq. (1) for each frequency component by the factors

$$\frac{\sin[\frac{1}{2}\omega_{JF_1F_2}(\delta x/v)]}{\frac{1}{2}\omega_{JF_1F_2}(\delta x/v)}\,\frac{\sin[\frac{1}{2}\omega_{JF_1F_2}(\Delta x/v)]}{\frac{1}{2}\omega_{JF_1F_2}(\Delta x/v)}\,, \qquad (2)$$

which show a reduction in the beat amplitude[5] with increasing $\delta x, \Delta x$.

On the other hand, to a good approximation, where $\tau v \gg \delta x, \Delta x$, the intensity of the emitted light increases linearly with $\delta x, \Delta x$ in our experiment. In order to find the best compromise between decreasing beat amplitude and increasing light intensity we apply the optimization criterion of Wittmann,[6] that $\sqrt{I}A$ (I is the intensity, A the modulation amplitude) should be a maximum. We thus multiply Eq. (2) by $(\delta x)(\Delta x)$ and meet the criterion for $\delta x = \Delta x = 2.33\ v/\omega_{JF_1F_2}$, where further complications in the determination of Δx due to the solid angle of the detection[6] have been neglected.

III. EXPERIMENTAL SETUP

The experimental setup is shown in Fig. 1. The incoming 330-keV $^{14}N^+$ beam passes through a diaphragm 0.2×8 mm and is then bent by electric field plates ($E \sim 2.8$ kV/cm) onto a polycrystalline Cu target of length $\delta x = 5.5$ mm. The target was cut from a CO_2 laser mirror with a surface roughness specified by the manufacturer to be ≤ 4 nm. The target length was chosen according to the discussion in the preceding chapter for expected hf frequencies of about $\nu = 100$–200 MHz (see Sec. VII).

The center of the target was positioned 3.5 mm below the incoming beam axis. The tilt angle of the target, with respect to the beam axis, was adjusted with the aid of a laser beam to about 1° with the intention that the beam will hit the target at an angle of about 1° and will be scattered by about 2° in order to travel parallel to the axis of the incoming beam after the interaction.

For purposes of normalization white light from the beam is detected 10 mm behind the target with an EMI multiplier via a flexible light guide.

As indicated in Fig. 1, diaphragm, field plates, target, and light guide are mounted on a common block which can be moved along the beam axis by a stepping motor drive.

With the aid of two stainless-steel wires of 0.2-mm diameter, the current profile of the beam after IBSIGI is monitored in both vertical and horizontal directions. It is shown below that one can accurately deduce from these profiles the geometry of the setup.

The detection zone has a length $\Delta x = 2.0$ mm. The circularly polarized light is detected through a rotatable achromatic quarter-wave plate, a linear polarizer, and a fused quartz lens ($f = 100$ mm). These image the 2-mm entrance slit of a Mod 218 McPherson spectrometer 1:1 into a plane containing the beam axis. The multiplier is a cooled RCA-31034 tube with a dark count rate of about 5 counts/sec.

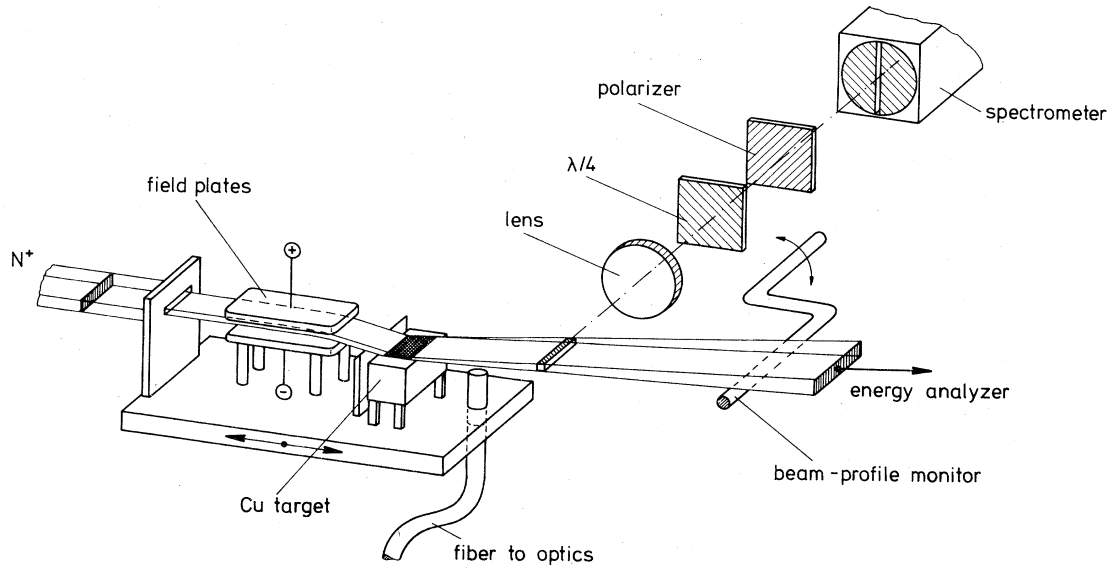

FIG. 1. Experimental setup.

The energy distribution of the scattered ions is measured with a 90° electrostatic energy analyzer with an energy resolution of about 10^{-3}. The calibration of this analyzer is known to be better than 10^{-3} by a direct comparison with a second analyzer of the same type previously calibrated by the He I $3p\,^3P$ quantum beats.[6]

IV. EXPERIMENT

For the experiment we chose the $2p3p\,^1P_1$ state of ^{14}N II where we expected, because of missing contact terms in the hf interaction, beat frequencies resolvable by the IBSIGI quantum-beat technique. From our former work[4] we estimated two frequencies of about 100 and 200 MHz. Furthermore, the lifetime of this state $\tau = 24.1$ nsec, as measured by Desesquelles,[7] is long enough to observe several periods of oscillations.

We observed the $2p3p\,^1P_1$ state via the $\lambda = 648.2$-nm $2p3s\,^1P_1^o$-$2p3p\,^1P_1$ transition with a maximum count rate of about 1000–2000 counts/sec. The other branch from this state, the $\lambda = 489.5$-nm $2s2p\,^1D^o$-$2p3p\,^1P_1$ transition, was weak and was not investigated owing to a blend with a line from N III at $\lambda = 486$ nm.

The quantum-beat structure in Fig. 2 was obtained by recording the intensity of the spectrally analyzed, circularly polarized light of positive and negative helicities I^+, I^- as the distance between the target and the fixed detection zone was varied in steps of 1 mm. At each step the quarter-wave plate was rotated to two positions as to successively accumulate I^- and I^+-photon counts into two separate memory blocks of a PDP 11/10 minicomputer synchronized with the target position. The spectrometer was set at $\lambda = 648.0$ nm with a resolution of $\Delta\lambda = 5$ nm at 2-mm slit width. Choosing the z axis as the quantization axis and the direction of detection, we get from Eq. (1) for the normalized Stokes parameter $S/I = (I^- - I^+)/(I^- + I^+)$,

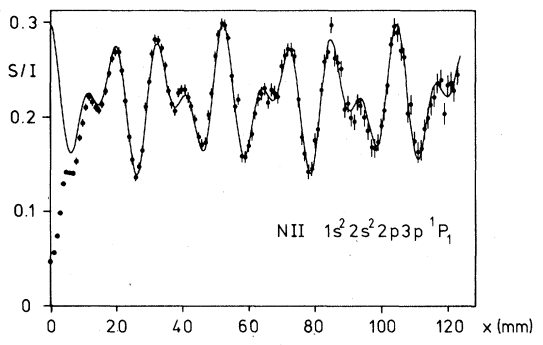

FIG. 2. Normalized Stokes parameter S/I as function of the distance between excitation and detection zone.

$$S/I(t) = \frac{\sqrt{3}(9 + 4\cos\omega_{10}t + 5\cos\omega_{21}t)\rho_0^1}{-36\sqrt{2}\rho_0^0 + (5 + 4\cos\omega_{20}t + 9\cos\omega_{21}t)\rho_0^2} . \quad (3)$$

Since ρ_0^0 exceeds ρ_0^2 by a factor of about 10 and the oscillatory part in the denominator of Eq. (3) is damped according to Eq. (2) by factors of 0.57 (ω_{21}) and 0.15 (ω_{20}) at our experimental conditions, the modulation amplitude due to the alignment is in the order of 0.5%. Thus it is justified to neglect the contribution of the alignment in the denominator of Eq. (3).

Therefore in using the normalized Stokes parameter S/I the influence of the exponential decay is eliminated and we have the modulation on a flat background. The beat pattern in Fig. 2 shows the superposition of two frequencies. The first part of the curve is disturbed by light emitted in the surface region where the contribution of atoms is considerable, which have experienced large scattering angles and consequently show small polarization.[2] These data are therefore omitted in the analysis.

V. RESULTS

The solid line in Fig. 2 is a best fit to the data using a function of the type

$$S/I(x) = a_0 + a_1\cos(a_2 x + a_3) + a_4\cos(a_5 x + a_3) \quad (4)$$

resulting from Eq. (3); a_0 describes a flat background, a_1 and a_4 the amplitudes of the "frequencies" a_2 and a_5.

In the final stage of the evaluation a_2 and a_5 were replaced by appropriate expressions containing the hf parameters A and B. For a $^1P_1$ state we have $a_2 = A - \frac{15}{4}B$ and $a_5 = 2A + \frac{3}{2}B$.

The fit yields for the hf constants, in reciprocal length units, $A' = 4.937 \times 10^{-2}$ mm^{-1} and $B' = -2.198 \times 10^{-3}$ mm^{-1}. These values of A' and B' are equivalent to two observable frequencies of 5.76×10^{-2} and 9.54×10^{-2} mm^{-1}, respectively, which correspond to the prominent features (lines) in the Fourier transform of the data in Fig. 3. In extracting these results from the data we have neglected a maximum possible shift of the observed frequencies of about 5×10^{-5} mm^{-1} due to the earth's magnetic field.

The ratio $a_1/a_4 = 1.18$ of the beat amplitudes of these two components resulting from the fitting procedure as well as from the Fourier transform deviates from the theoretical value 0.80 as given in Eq. (3). Including the correction due to the finite length of the excitation and detection zone, however, the theoretical value shifts to 1.20, which is in good agreement with the experiment.

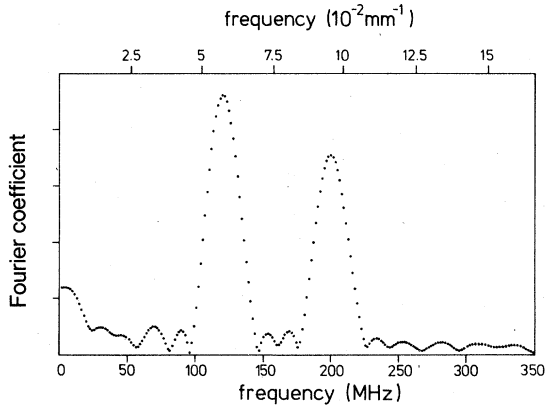

FIG. 3. Fourier transform (sinusoidal apodisation) of the data in Fig. 2.

VI. VELOCITY DETERMINATION

The conversion of the hf parameters into frequency units via $A = A'v, B = B'v$ requires knowledge of the average velocity v of the atoms after the ion-solid interaction.

Since the energy loss in the ion-solid interaction depends on the scattering angle of the ions, a detailed analysis of the scattering under our experimental conditions is necessary for a reliable determination of this average velocity. Figure 4 displays the geometry of that part of the setup which is of interest for the study of the scattering process.

The incoming $^{14}N^+$-beam first passes through a diaphragm 0.2×8 mm and is then bent away from the original beam axis and onto the target by two electric field plates. At a distance $l_1 = 70$ mm behind the target the vertical current distribution of the ions is scanned by a thin wire along the y axis. The resulting curve (Fig. 4) is marked by two strong peaks in the current distribution. One peak at $y = d_1$ stems from the fraction of neutralized atoms which are not deflected by the electric field and thus defines the axis of the incoming beam. (The current picked up by the wire is due to secondary electron emission and to the fraction of the neutral beam which has been ionized by the back ground gas between the field plates and the wire.) The other peak at $y = 0$ is generated by those ions missing the target without interaction and deflection.

From these two vertical positions—separated by a distance $d_1 = 6.4$ mm—one deduces a bending of the incoming beam by arctan $[d_1/(l_1 + l_2)] = 2.4°$ ($l_2 = 86$ mm), which is consistent with a calculation taking into account the geometry of the field plates and an applied voltage of 1400 V.

The distribution of scattered ions starts at a position $y = d_2$, where the wire lies in the plane of the target surface and ions with the smallest possible scattering angle are detected. From $y = d_2$ an angle of incidence of the ions onto the target surface of 1.2° can be deduced.

The maximum of the distribution of the ion current at $y = d_3$ corresponds to a scattering angle of 2.8° and verifies an earlier observation[2] that the exit angle at maximum (1.6°) exceeds the angle of incidence (1.2°).

The angular spread of the surface scattered-ion current in the y direction has a FWHM of 3.2°.

The limited angular acceptance of the energy

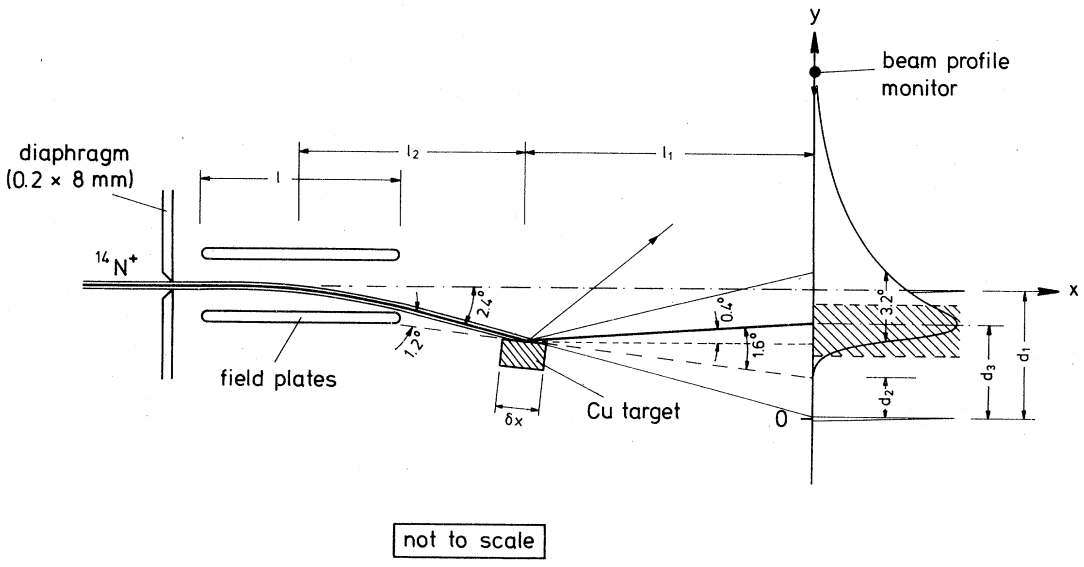

FIG. 4. Vertical scattering of ions.

analyzer used for the energy measurement of the scattered ions is also shown in Fig. 4. Since the overlap is smaller than the angular FWHM, one has to determine the average velocity of the scattered ions by taking into account the dependence of the energy loss on the scattering angle.

In order to obtain information on this dependence the current pickup wire was replaced by a horizontal slit of 0.2 mm width and the energy distributions for different scattering angles in the angular acceptance of the energy analyzer were recorded. A typical scan recorded sweeping the high voltage of the energy analyzer is shown in Fig. 5.

With the energy of the incoming beam E_0, the mean and the maximum energies E_{mean}, E_{max} of this distribution define two energy losses $\eta_{mean} = E_0 - E_{mean}$ and $\eta_{max} = E_0 - E_{max}$. For the angular range under study we find for both η_{mean} and η_{max} a linear dependence on the scattering angle. This is a result which agrees for the latter with a postulate given by Marwick *et al.*[8]

The linear change of η_{mean} by 2 keV/deg scattering angle weighted with the angular intensity distributions in Fig. 4 yields an averaged energy of $E = 318.0$ keV.

The surface scattering in the horizontal plane—measured in the same way along the z axis as the vertical distribution along the y axis—is significantly smaller and η^z_{mean} changes only by about 1 keV/deg. This z component of the surface scattering was taken into account by a reduction of E by 2.0 keV.

As the final result we get for the average energy after the target interaction $E_{av} = 316.0 \pm 6.0$ keV as compared to the actual mean energy $E_{mean}(\text{exp}) = 322.2$ keV measured with the angular acceptance indicated in Fig. 4 during the quantum-beat measurements. The rather large uncertainty at E_{av} of 2% stems from our conservative estimates of possible sources of error inherent in the averaging procedure applied.

As shown in Fig. 2 the reduction in the beat amplitude with increasing distance from the target is almost negligible. This can be understood as a further justification for our averaging procedure since it clearly indicates that the contribution of low-energy ions to the total energy distribution is small.

VII. DISCUSSION

From E_{av} we derive the average velocity $v_{av} = 2.085 \pm 0.020$ mm/nsec and calculate our final results for the hyperfine structure constants $A = A'v_{av} = 102.9 \pm 1.0$ MHz and $B = B'v_{av} = -4.58 \pm 0.05$ MHz. (The direct determination of v_{av} from the velocity distribution is in principle the better approach but results—despite the asymmetric line shape—in a negligible deviation from the value derived from E_{av}.)

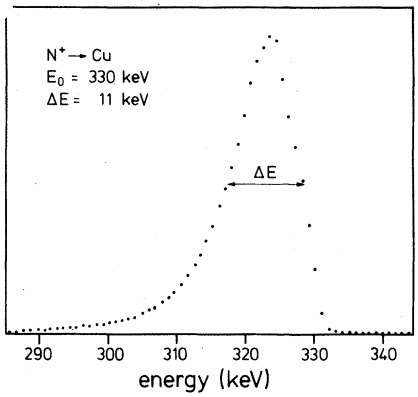

FIG. 5. Energy distribution of ions after the target interaction.

From a single-configuration Hartree-Fock calculation[9] one obtains for the $2p3p\ ^1P_1$ configuration $\langle r^{-3}\rangle_{2p} = 4.694 a_0^{-3}$ and $\langle r^{-3}\rangle_{3p} = 0.389 a_0^{-3}$. The agreement of the A factor $A = 97.9$ MHz, deduced from these integrals, with the experiment is satisfactory.

An important aspect of our measurement is the fact that the measured A and B factors allow a determination of the quadrupole moment of ^{14}N $Q(^{14}\text{N})$, exceeding the precision of previous results.

Since the ground state of the neutral ^{14}N atom is a ^4S state, even precise magnetic-resonance experiments are unable to deduce the quadrupole moment.[10] Therefore, $Q(^{14}\text{N})$ has previously been determined for the most part from data of hf splittings in molecules where uncertainties in the theoretical description cause errors in the extracted value for $Q(^{14}\text{N})$ of about 40% or more.

In order to derive the quadrupole moment $Q(^{14}\text{N})$ from our measurement on N II $1s^2 2s^2 2p3p\ ^1P_1$, we consider the two-electron system $2p, 3p$.

For the magnetic dipole interaction a Hamiltonian of the form[11]

$$\mathcal{H} = \sum_{i=1}^{N} [l_i a_l - \sqrt{10}(s \times C^2)^1_i a_{sd} + s_i a_s] \vec{I}$$

is normally used. For the configuration under study only the orbital operator with

$$a_l = 2\mu_B \mu_I / I \langle r^{-3}\rangle_l$$

is relevant, where μ_B is the Bohr magneton and $\mu_I = 0.4037 \mu_B m_e/m_p$ (Ref. 12).

Following the discussion of Rosén[13] we first have to derive the quadrupole moment on the base of unrestricted wave functions from $\langle r^{-3}\rangle_{nl}$ and then apply the Sternheimer correction.

Since the relativistic correction factors for

nitrogen are small[14] with respect to the uncertainty inherent in the Sternheimer correction, we do not account for relativistic effects and determine $\langle r^{-3}\rangle_{nl}$ directly from the measured magnetic hf constant.

For a two-electron system (l_1, l_2) we have the A factor

$$A_J=\left(\frac{2J+1}{J(J+1)}\right)^{1/2}(2L+1)(-1)^{J+l_1+l_2}\begin{Bmatrix} J & L & S\\ L & J & 1\end{Bmatrix}\times\left[\begin{Bmatrix} L & L & 1\\ l_1 & l_1 & l_2\end{Bmatrix}[l_1(l_1+1)(2l_1+1)]^{1/2}a_{n_1l_1}+\begin{Bmatrix} L & L & 1\\ l_2 & l_2 & l_1\end{Bmatrix}[l_2(l_2+1)(2l_2+1)]^{1/2}a_{n_2l_2}\right]$$

and for $^1P_1(l_1=l_2=1)$ in particular,

$$A=0.5(a_{2p}+a_{3p}).$$

We thus obtain for the sum of the radial integrals:

$$\langle r^{-3}\rangle_{2p}+\langle r^{-3}\rangle_{3p}=AI/\mu_B\mu_I=5.352\pm0.052a_0^{-3}.$$

The B factor for a two-electron system is

$$B=(-1)^{J+s+l_1+l_2+1}2(2J+1)(2L+1)\begin{pmatrix} J & 2 & J\\ -J & 0 & J\end{pmatrix}\begin{Bmatrix} J & L & S\\ L & J & 2\end{Bmatrix}\times\left[\begin{Bmatrix} L & l_1 & l_2\\ l_1 & L & 2\end{Bmatrix}(-1)^{l_1}(2l_1+1)\begin{pmatrix} l_1 & 2 & l_1\\ 0 & 0 & 0\end{pmatrix}b_{n_1l_1}+\begin{Bmatrix} L & l_2 & l_1\\ l_2 & L & 2\end{Bmatrix}(-1)^{l_2}(2l_2+1)\begin{pmatrix} l_2 & 2 & l_2\\ 0 & 0 & 0\end{pmatrix}b_{n_2l_2}\right],$$

with $b_{nl}=e^2Q\langle r^{-3}\rangle_{nl}$.

For the $2p3p\,^1P_1$ configuration Eq. (4) reduces to

$$B=-0.2(b_{2p}+b_{3p}),$$

so that we obtain the so-called "experimental" quadrupole moment

$$Q(^{14}\mathrm{N})=-5B/e^2(\langle r^{-3}\rangle_{2p}+\langle r^{-3}\rangle_{3p})^{-1}=18.22\pm0.27\ \mathrm{mb},$$

assuming that $\langle r^{-3}\rangle_{2p}$ and $\langle r^{-3}\rangle_{3p}$ are the same for the magnetic dipole and electric quadrupole hf interaction. That is, we neglect magnetic-shielding effects.

For the configuration under study, Sternheimer[15] estimates a shielding factor of $R=0.06\pm0.04$, so that the corresponding correction[15] factor $C=1/(1-R)$ for the quadrupole moment is 1.06 ± 0.04. Hence we finally obtain the quadrupole moment of ^{14}N:

$$Q(^{14}\mathrm{N})=19.3\pm0.8\ \mathrm{mb}.$$

In Table I we compare our result with values obtained from molecular physics.

TABLE. I. Zero-field quantum-beat quadrupole moment compared with various molecular-physics values.

Molecule atom	$Q(^{14}\mathrm{N})$mb
NO[a]	16 ± 7
N_2[b]	21.5
	17.9–22.4
FCN[c]	15.7
NF_3[d]	10
ClCN[e]	16.1
	~20
HCCN[f]	16.6
NH_3[g]	8.9–22
	8.9–16.6
	15.1
N_2 (solid)[h]	14.7
R-CN ("average")[i]	16.6
"average"[j]	15.6
BrCN[k]	~20
N^+[l]	19.3± 0.8

[a] Ref. 19.
[b] Kapral and Allen, Richardson, Ransil, see Ref. 15.
[c] McLean and Yoshimine, see Ref. 15.
[d] Ref. 20.
[e] McLean and Yoshimine, see Ref. 15; Ref. 21.
[f] McLean and Yoshimine, see Ref. 15.
[g] Kaldor and Shavitt; Kern; Fink and Allen, see Ref. 15; Ref. 17.
[h] Kern; Kern and Karplus, see Ref. 15.
[i] Ref. 16.
[j] Ref. 17
[k] Ref. 21.
[l] This work.

Although no error limits are given in most cases, the uncertainty of the Q values in Table I should be considerable for those values which have been derived with the help of computed electric field gradients. Attempts of listing "average values" for $Q(^{14}\mathrm{N})$, as derived from different molecules, have been made by Bonaccorsi *et al.*[16] and by O'Konski and Ha[17] to yield $Q=16.6$ and 15.6 mb, respectively. Although the latter authors quote an estimated uncertainty of ±5% in a later publication,[18] the discrepancy with our result may still be due to the principle difficulty of using computed electric field gradients.

The only value derived from molecular quadrupole constants in NO without the necessity of computing the electric field gradient is given by Lin[19]: $Q=16\pm7$ mb. This value is in agreement with our result. Hence one cannot conclude at present that a fundamental discrepancy exists between the values of Q derived from molecular and atomic hfs measurements. It is, however, evident that the "atomic" value exceeds the "molecular" ones with respect to accuracy and reliability.

VIII. CONCLUSION

We have measured the hf structure of ^{14}N II $2p3p\ ^1P_1$ by the zero-field quantum-beat technique after interaction of fast ions with a surface at grazing incidence.

We determined the hyperfine interaction constants $A = 102.9 \pm 1.0$ MHz and $B = -4.58 \pm 0.05$ MHz, from which we deduce the nuclear quadrupole moment of ^{14}N to be $Q(^{14}\mathrm{N}) = 19.3 \pm 0.8$ mb with improved accuracy in comparison to previous values. An extensive theoretical treatment of the configuration under study will certainly reduce the uncertainty in $Q(^{14}\mathrm{N})$. While the error limit of Q is due mainly to the uncertainty of the Sternheimer correction, the experimental error limit of ±1% for the hf interaction constants stems predominantly from the uncertainty in the determination of the average velocity of the surface scattered ions.

In order to improve the experimental situation for future applications of this IBSIGI quantum-beat technique one can use a smaller angle of incidence and a target material with higher Z. Both lead to a considerable reduction of the angular and energy spread after surface scattering.[22] An even further reduction of these spreads is obtained for ions of higher nuclear charge Z. Hence, based on the universal production of large anisotropy by IBSIGI, one can expect the IBSIGI quantum-beat technique to be very well suited for hfs studies with an accuracy of a few parts per thousand. It may be applied to any state with hf beat frequencies in the range studied here, if the emitted radiation can be analyzed with respect to its circular polarization.

ACKNOWLEDGMENTS

We wish to thank Professor R. M. Sternheimer for his communication and A. Gaupp for performing the single-configuration hf calculation. The various supports of A. Hensel, R. Burghardt, G. Sedatis, and D. Kline, the assistance of N. Kirchner and R. Rauchfuss during the measurements, and the critical reading of the manuscript by E. Myers (Oxford) are gratefully acknowledged.

[1] H. J. Andrä, Phys. Scr. 9, 257 (1974).
[2] H. J. Andrä, Phys. Lett. A 54, 315 (1975); H. J. Andrä, R. Fröhling, H. J. Plöhn, and J. D. Silver, Phys. Rev. Lett. 37, 1212 (1976); H. J. Andrä, R. Fröhling, and H. J. Plöhn, in *Inelastic Ion-Surface Collisions*, edited by N. H. Tolk, J. C. Tully, W. Heiland, and C. W. White (Academic, New York, 1977); H. G. Berry, G. Gabrielse, A. E. Livingston, R. M. Schectman, and J. Desesquelles, Phys. Rev. Lett. 38, 1473 (1977); H. G. Berry, G. Gabrielse, and A. E. Livingston, Phys. Rev. A 16, 1915 (1977).
[3] H. J. Andrä, H. J. Plöhn, A. Gaupp, and R. Fröhling, Z. Phys. A 281, 15 (1977).
[4] H. J. Andrä and H. Winter, Hyperfine Int. 5, 403 (1978).
[5] H. J. Andrä, in *Progress in Atomic Spectroscopy*, Part B, edited by W. Hanle and H. Kleinpoppen (Plenum, New York, 1979), p. 829.
[6] W. Wittmann, Ph.D. thesis, Free University, Berlin, 1977 (unpublished).
[7] J. Desesquelles, Ann. Phys. (Paris) 6, 71 (1971).
[8] A. D. Marwick, M. W. Thompson, B. W. Famery, and G. S. Harbinson, Radiat. Eff. 10, 49 (1971).
[9] C. Froese-Fischer, Comput. Phys. Commun. 4, 107 (1972).
[10] J. M. Hirsch, G. H. Zimmermann III, D. J. Larson, and N. F. Ramsey, Phys. Rev. A 16, 484 (1977).
[11] L. Armstrong, Jr., *Theory of the Hyperfine Structure of Free Atoms* (Wiley-Interscience, New York, 1971).
[12] Y. Ting and B. Williams, Phys. Rev. 89, 595 (1953).
[13] A. Rosén, Phys. Scr. 8, 159 (1973).
[14] H. Kopfermann, *Nuclear Moments* (Academic, New York, 1958).
[15] R. M. Sternheimer (private communication); Phys. Rev. 84, 244 (1951); 164, 10 (1967); Phys. Rev. A 6, 1702 (1972); R. M. Sternheimer and R. F. Peierls, *ibid.* 4, 1722 (1971), and references therein.
[16] R. Bonaccorsi, E. Scrocco, and J. Tomasi, J. Chem. Phys. 50, 2940 (1969).
[17] C. T. O'Konski and T. K. Ha, J. Chem. Phys. 49, 5354 (1968).
[18] C. T. O'Konski and T. K. Ha, J. Chem. Phys. 56, 3169 (1972).
[19] C. C. Lin, Phys. Rev. 119, 1027 (1960).
[20] J. Sheridan and W. Gordy, Phys. Rev. 79, 513 (1950).
[21] C. H. Townes, A. N. Holden, and F. R. Merritt, Phys. Rev. 74, 1113 (1948).
[22] N. Kirchner, H. Winter, and H. J. Andrä, report on spring meeting of the DPG, Berlin, 1979 (unpublished).